Predictions in a data-sparse region using a regionalized grid-based hydrologic model driven by remotely sensed data

Luis Samaniego, Rohini Kumar and Conrad Jackisch

ABSTRACT

The goal of this study was to assess the feasibility of using Tropical Rainfall Measuring Mission (TRMM) and Moderate Resolution Imaging Spectroradiometer (MODIS) products to drive a mesoscale hydrologic model (mHM) in a poorly gauged basin. Other remotely sensed products such as LandSat and Shuttle Radar Topography Mission (SRTM) were also used to complement the local geoinformation. For this purpose, three data blending techniques that combine satellite with *in situ* observations were implemented and evaluated in the Mod basin (512 km^2) in India. The climate of the basin is semi-arid and monsoon-dominated. The rainfall gauging network comprised six stations with daily records spanning 9 years. Daily discharge time series was only 4 years long and incomplete. Lumped and distributed versions of mHM were evaluated. Parameters of the lumped version were obtained through calibration. A multiscale regionalization technique was used to parameterize the distributed version using global parameters from other gauged basins. Both mHM versions were evaluated during six monsoon seasons. Results of numerical experiments indicated that driving mHM with satellite-based products is possible and promising. The distributed model with regionalized parameters was at least 20% more efficient than that of its lumped version. Initialization conditions must be carefully considered when the model is only driven by remotely sensed inputs.

Key words | data-sparse region, mHM model, PUB, regionalization, remote sensing

Luis Samaniego (corresponding author)
Rohini Kumar
UFZ-Helmholtz-Centre for Environmental Research,
Leipzig,
Germany
E-mail: *luis.samaniego@ufz.de*

Conrad Jackisch
Technical University of Munich,
Munich,
Germany

INTRODUCTION

Most river basins of the world are currently either poorly gauged or totally ungauged in some respect, either because a required variable has not been sampled at the required resolution or because it has not been observed during a period of interest (Sivapalan *et al.* 2003). Furthermore, the number of hydrological monitoring facilities has declined rapidly (Vorosmarty 2001) during the last decades, mainly due to lack of funds or unwillingness of state authorities to keep functioning monitoring networks. Developing countries have been the most affected in this respect.

The advancement of techniques aimed at performing predictions and forecasts at ungauged and poorly gauged locations is a major challenge in hydrology. This is mainly because decisions for the design of infrastructure and water resources management affecting millions of human beings, biodiversity and non-renewable natural resources often require robust estimates of key hydrologic variables. Moreover, risks related to extreme hydrological events are steadily increasing almost everywhere due to land cover/use and climatic changes, as well as population growth (Solomon *et al.* 2007).

For water resources planning and design of engineering structures, there is a need for hydrologic projections and simulations. These can only be obtained with a reliable hydrologic model, whose complexity should be carefully considered based primarily on data availability and its intended application. In many poorly gauged or ungauged regions, however, the application of even the simplest kind of hydrologic model is often not possible either because: (1) there are no sufficient hydrometeorological records available which

doi: 10.2166/nh.2011.156

are required to achieve a robust model parameterization; or (2) because the required inputs (e.g. precipitation, temperature) are not available in the meteorological records during the period of interest, or both. The following alternatives can still be an option in such situations.

First, in the case that a model could not be calibrated in a given basin, model parameters may be transferred from similar gauged basins as suggested by McIntyre *et al.* (2005) and Samaniego *et al.* (2010a). Transferring parameters from a gauged to an ungauged basin is, however, a difficult undertaking because calibrated effective parameters tend to compensate for deficiencies in the model structure (Xia *et al.* 2002). Lumped models are the simplest ones with respect to the number of parameters, and often used in this situation (Wagener & Wheater 2006; Oudin *et al.* 2008). Lumped models, however, completely lack the spatial representation of the basin characteristics which may be quite important when parameters are transferred from one basin to another (Bárdossy 2007). For this reason, special consideration should be given to the spatial heterogeneity of the basin characteristics and their influence in the characterization of the dominant hydrologic process (Kirchner 2006).

Distributed models, on the contrary, require distributed inputs which are not always available. Moreover, there is still controversy over the efficiency and applicability of distributed models in practical applications (Reed *et al.* 2004). Regionalization techniques have been pursued in hydrological modelling (Abdulla & Lettenmaier 1997; Hundecha & Bárdossy 2004; Pokhrel *et al.* 2008) not only to address deficiencies of existing distributed models (e.g. overparameterization) but also to facilitate the transferability of parameters across scales and locations. Existing regionalization techniques, however, do not explicitly account for the sub-grid variability of basin descriptors; these, in turn, affect water fluxes and their spatial–temporal patterns. A recently developed multiscale regionalization technique addresses these issues explicitly (Samaniego *et al.* 2010b). This technique was employed in this study.

Second, in the case that meteorological records are not available, forcings derived from remotely sensed products may be used to drive a model during a period of interest. Currently, there is a plethora of satellite missions dedicated exclusively to observe variables relevant for land surface hydrology at a global scale.

Precipitation, for instance, has been the main focus of a number of satellite missions during the last four decades, among them: Defense Meteorological Satellites Program (DMSP), National Oceanic and Atmospheric Administration (NOAA), Advanced Microwave Scanning Radiometer (AMSR-E), Moderate Resolution Imaging Spectroradiometer (MODIS)-Aqua, Geostationary Operational Environmental Satellites (GOES) and Tropical Rainfall Measuring Mission (TRMM).

Based on these data, precipitation products with a temporal resolution of 30 minutes and a grid resolution of about 8 km at the equator have been derived with the CMORPH (Climate Prediction Center morphing) technique (Joyce *et al.* 2004). Other important variables such as land surface temperature, atmospheric temperature and leaf area index are currently acquired, for example, by MODIS satellites (Aqua and Terra) with a spatial resolution of 1 km. Cloud water, near-surface wind speed, soil moisture and snow cover are currently measured by a number of weather satellites such as AMSR-E and NOAA.

The major advantage of satellite products with respect to meteorological stations is their spatio-temporal coverage. Thus, satellite data may be the only available products to study the weather, climate and hydrology in most regions with sparse networks. The quality of these satellite products for hydrologic applications is still in dispute, however, because of its coarseness and intrinsic bias (Hossain & Huffman 2008; Tobin & Bennett 2010). So far, very few studies have investigated the quality of these products for hydrologic predictions in data-sparse or ungauged semi-arid regions.

Within this framework, this study investigates three main research questions. (1) Is it advantageous to apply a lumped model in a data-sparse basin instead of a regionalized distributed hydrologic model? (2) How reliable is a satellite precipitation product (e.g. TRMM) for hydrologic predictions in a poorly gauged basin? (3) Under which conditions can remotely sensed data be used to drive a hydrological model in a data-sparse region?

These three research questions were addressed in corresponding numerical experiments, including sensitivity analysis to guarantee the reliability of the testing procedure. A semi-arid basin in northwest India (the Mod basin) was selected as a study area because of its extreme meteorological

conditions and relatively good availability of morphological data, but poor hydro-meteorological information.

STUDY AREA

General description

The Mod basin covers an area of 512 km^2 in a semi-arid rural landscape located in the western Plateau and Hills region, northwest India (Figure 1). The Mod river is an ephemeral headwater tributary of the Mahi river whose elevation ranges from 230 to 590 m with a mean elevation of 380 m a.s.l. Although this region is sparsely inhabited, it has endured drastic deforestation during the last decades. In the 1960s, about 33% of this area was covered by dense forest while in the early 1990s, a mere 5% of the basin's area was still covered by forest (Jackisch 2007). Climate of the basin is semi-arid according to Köppen notation, with well-defined seasons. Summers are hot, winters are short, and the monsoon season (June–September) brings almost 80% of the annual rainfall with an average of 800 mm. As a result of these climatic conditions, the soil moisture regime is ustic (i.e. dryness). The geology of the catchment is mainly composed of Precambrian igneous and Cretaceous sedimentary formations, with shallow and stony soils. Major soil texture classes are clay and clay loam.

Data availability

1. Daily precipitation is available for six rainfall gauges (Figure 1) from the beginning of 1992 until the end of 2000. Daily maximum and minimum air temperature are available from only one meteorological station (Indore station) for the period from 01/01/1992–31/08/2001. This station is located about 100 km away from the study area.
2. Daily discharge is available for one gauging station at Mod-kheri (Figure 1) during the period 1992–1996. This time series contains about 10% missing values. This information is less reliable than the meteorological information due to the lack of maintenance of the gauging station and the harsh meteorological conditions.
3. Land cover data was derived from a 1993 Landsat TM5 scene (30 m × 30 m) (http://landsat.gsfc.nasa.gov/). The method of maximum likelihood was used to classify

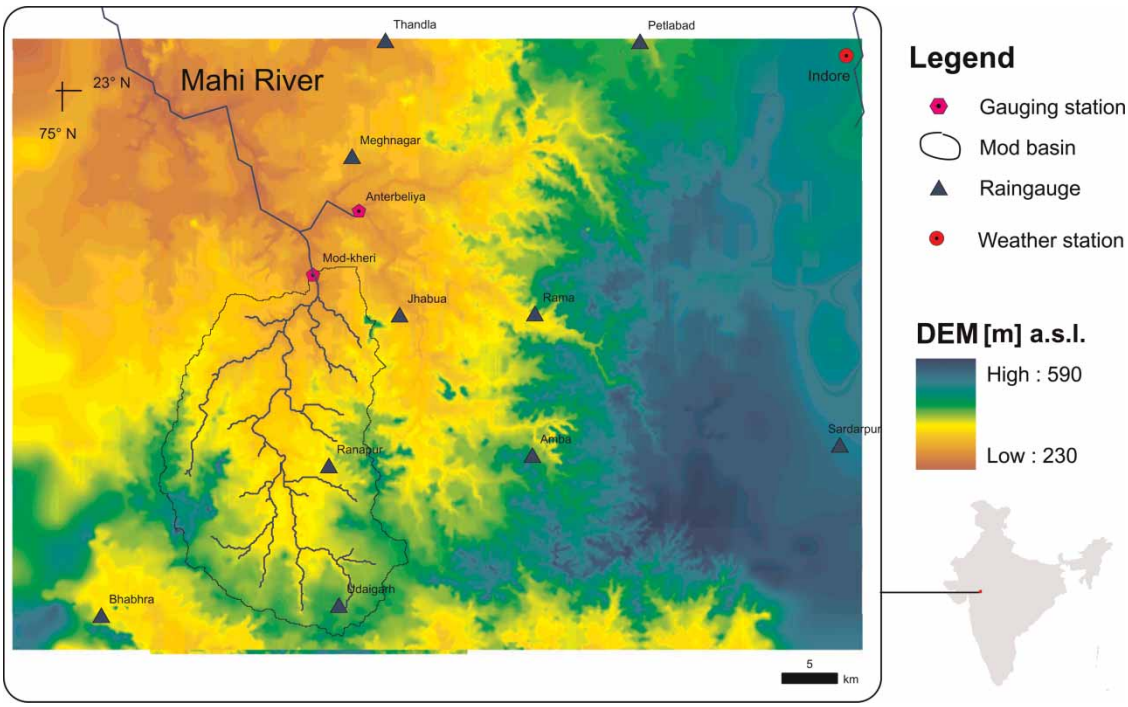

Figure 1 | Location of the Mod Basin.

this scene using 73 ground-truth samples obtained during a field trip. Old topographic maps and local expertise were also employed to determine ground-truth locations, which most likely did not endure land cover changes. Such locations included inner forested areas, wastelands, floodplains and traditional farmlands. The user accuracy obtained with this procedure was on average 0.70 for the three main land cover classes (Jackisch 2007), namely: forest, impervious surfaces and permeable surfaces that comprise fallow lands or those surfaces covered by crops, grass and wetlands.

4. Terrain elevation was obtained from the SRTM sensor (NASA) with a spatial resolution of 90 m × 90 m. This data was obtained freely from http://srtm.csi.cgiar.org/.
5. Soil texture at different horizons and the geological formations were obtained from digital maps at the scale of 1:250,000 (Geological Survey of India 1978).
6. Daily precipitation was obtained from the TRMM (level 3B-42) (http://trmm.gsfc.nasa.gov/) with a spatial resolution of 25 km × 25 km for the period from 1998 to 2008.
7. Day and night land surface temperatures (LST) were obtained from MODIS, NASA, with a spatial resolution of 1 km × 1 km for the period from 2001 to 2008. These data are available freely from https://wist.echo.nasa.gov/api/.

DATA BLENDING, MODELLING AND PARAMETER REGIONALIZATION

Blending remote sensing data with *in situ* observations

There are many attempts reported in the literature in which various sources of remotely sensed products have been merged with the aim of producing a blended product which enhances the characteristics of its individual components. For example, a blended product can be created by combining Landsat (30 m × 30 m, revisit rate 16 days) and MODIS (1,000 m × 1,000 m revisit rate 6 hours). This new product takes advantage of the spatial detail of Landsat and the temporal regularity of MODIS acquisitions. As a result, high-resolution Normalized Difference Vegetation Index (NDVI) or Leaf Are Index (LAI) imagery can be generated over a growing season to reveal phenological patterns (Hilker *et al.* 2009; Samaniego *et al.* 2010b). Another interesting example is the combination of various passive microwave and infrared data to produce global precipitation estimates (Joyce *et al.* 2004).

In this study, various techniques (e.g. External Drift Kriging) were pursued to create daily precipitation, temperature, and potential evapotranspiration fields with a spatial resolution of 1,000 m. These fields are required as forcings for a distributed hydrologic model. In general, these techniques aimed at blending remotely sensed data with *in-situ* observations either to reduce the inherent uncertainty of the former or to better represent the spatial variability of the observed variable.

External Drift Kriging (EDK) is a geostatistical interpolation technique to estimate the value of a random variable at an unsampled location given a set of observations and additional knowledge called the external drift (Deutsch & Journel 1998). This method assumes that the expectation of a given random variable is not constant over the domain of interest and that the variance of the increment corresponding to two different locations depends only on the magnitude of the vector separating them, which is denoted by the variogram function γ. EDK should be used in those cases in which the expectation of the random variable over the domain of interest is non-stationarity.

The main difference between kriging and other interpolation techniques is that it ensures that the estimated value has both zero bias (i.e. the unbiased condition) and the smallest possible estimation variance. The random variable at an unknown location $\hat{Z}(\mathbf{x})$ can be estimated as a linear combination of the existing observations $\{Z(\mathbf{x}_i),\ i = 1, \ldots, n\}$ where n is the sample size. The weights associated with each observation can be found in such a way that the unbiased estimator has the smallest possible estimation variance. For more details, refer to Deutsch & Journel (1998).

Precipitation fields

Precipitation is quite likely the most important factor governing the water balance of a region (Pan *et al.* 2010). Its occurrence and spatial distribution are therefore key elements in understanding the water cycle at basin level. Unfortunately, dense raingauge/radar networks are only

available in developed regions; most of the Earth's land surface remains ungauged or, at best, covered by sparse networks. A number of precipitation products providing global coverage have therefore been derived from passive microwave sensors carried by low orbiter satellites (e.g. DMSP, NOAA, TRMM, GOES). Although their level of accuracy is still in dispute (Gebremichael *et al.* 2003; Hossain & Huffman 2008; Tobin & Bennett 2010), they have a major advantage compared to raingauge measurements since: (1) they provide a continuous estimate of the spatio-temporal variation of rainfall which may not be perceived by analysis of data from stations only (Kirchner 2006) and (2) they provide a reliable and systematic estimate of latent heat, which is a valuable information about the driving force behind weather systems (especially in the tropics).

We therefore hypothesized that these data sources may contribute to the generation of reliable streamflow predictions in data-sparse regions. In particular, we wish to determine whether a mixture of satellite and sparse raingauge data improves model predictions compared to satellite data alone. TRMM data were used to test this research objective for two reasons: it is one of the most accurate and comprehensive data sources available (Pan *et al.* 2010), and the acquisition dates of the TRMM data coincided with with *in situ* observations for a period of 3 years (i.e. 1998–2001).

Generating daily regional precipitation fields in data-sparse regions is usually quite difficult (if not impossible) because interpolation methods such as EDK require a robust estimate of the precipitation variogram; this can only be obtained in regions with a relatively dense observation network. In the study area, the variogram could not be inferred from the gauging stations because they are too few (only six stations).

Instead, we hypothesized that TRMM data can be used as a proxy to estimate the precipitation variogram since these observations offer a continuous coverage over the whole region (Figure 2(a)). The following procedure was used to blend TRMM data with that of the meteorological stations.

1. Extract TRMM data for a spatial domain covering the Mod basin (Figure 2(a)) over the period 01/01/1998–31/12/2008.
2. Use every cell within a selected domain of the TRMM field in a given period to estimate the experimental

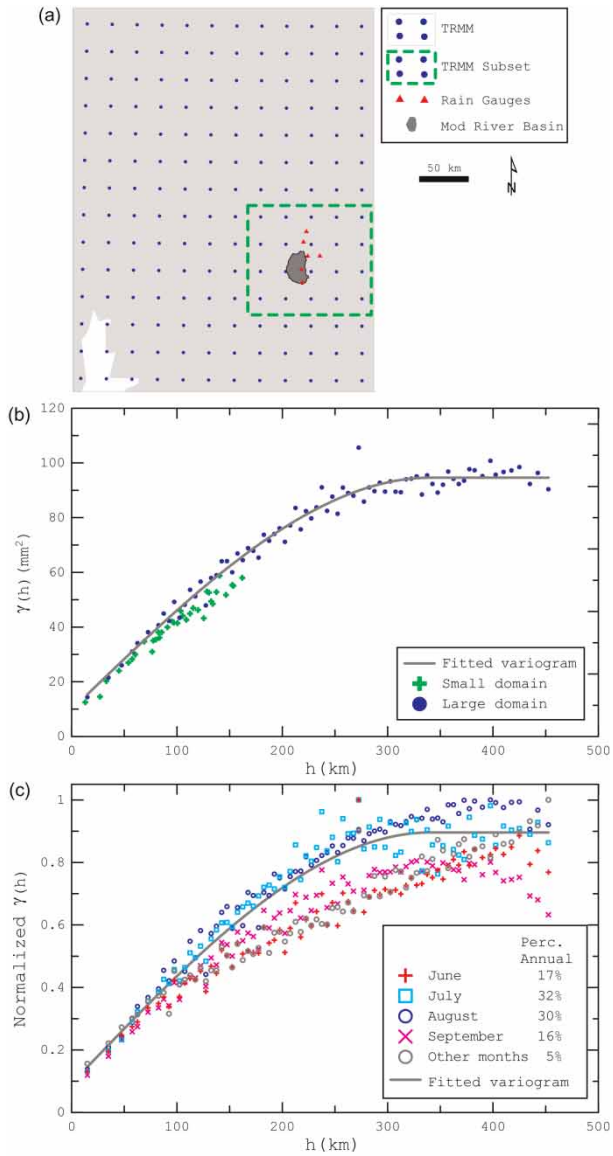

Figure 2 | (a) TRMM data used for the estimation of the variogram. (b) Variograms estimated in large and small spatial domains. (c) Normalized variograms estimated for the large spatial domain in different periods.

precipitation variogram. The variogram can be estimated as follows:

$$\gamma(h) = \frac{1}{2N_h} \sum_{||\mathbf{x}_i - \mathbf{x}_j|| = h} (Z(\mathbf{x}_i) - Z(\mathbf{x}_j))^2 \quad (1)$$

where N_h denotes the number of pairs of locations separated by a vector h and i, j denote a given pair of locations.

3. Fit a theoretical variogram to the empirical variogram obtained in step 2. The spherical variogram is typically used for precipitation fields. The equation of this variogram is given by

$$\gamma(h) = c_0 + \begin{cases} c\left(\frac{3}{2}\frac{h}{a} - \frac{1}{2}\left(\frac{h}{a}\right)^3\right) & h \le a \\ c & h > a \end{cases} \quad (2)$$

where c_0, c and a are parameters denoting the nugget, the sill and the range of the variogram. These parameters can be estimated by minimizing a robust estimator such as the L_1-norm (i.e. the sum of the absolute errors between the calculated and the observed variogram) with a non-linear optimization algorithm. Other types of theoretical variograms should be used (Deutsch & Journel 1998) if the correlation coefficient between the empirical and the theoretical variogram is too low (say, less than 0.5).

4. Estimate daily precipitation fields by EDK for unsampled locations (e.g. 1 km grid cell) in the study domain using the theoretical variogram obtained from TRMM data (steps 2 and 3) and the rainfall time series from the meteorological stations. The terrain elevation was used as an external drift.

Daily TRMM fields were also used to force the hydrological model to compare these results with those of the proposed blending method.

Tests to ensure the applicability of EDK

To ensure the applicability of EDK in the present study, the following conditions were tested: (1) the significance of the relationship between TRMM precipitation and terrain elevation; and (2) the spatial and temporal robustness of the variogram derived from the TRMM data.

The first condition is necessary to justify the applicability of EDK. If the correlation between the drift and the random variable is weak (say $r^2 < 0.3$) then ordinary Kriging would be adequate. In the present case, the relationship of daily precipitation and elevation was significant ($r^2 \sim 0.4$, p-value 0.05).

The second condition is important to reject the null hypothesis that the empirical variogram is valid only locally or for a small period. Two overlapping sets were selected to assess the spatial coherence of the empirical variogram as indicated in Figure 2(a).

Results of this analysis indicated that both variograms are highly correlated to one another within the range of 150 km (Figure 2(b)). The TRMM data were segregated into five periods to test the temporal invariance of the variogram. The first four correspond to those months which account for the 95% of the annual precipitation (i.e. the monsoon period), whereas the last included the remaining months. The spatial variability of the precipitation during July and August, which contribute about 60% of the annual precipitation, is similar (Figure 2(c)). The precipitation variability during June and September is different from the previous variograms for distances greater than 100 km. Since all variograms are practically the same for separation distances less than 100 km, a unique variogram can be used to interpolate the rainfall station data.

Temperature and potential evapotranspiration

Apart from precipitation, meteorological variables such as air temperature, relative humidity and wind speed, among others, are also fundamental to understanding the water balance of a region. The spatio-temporal distribution of these variables is highly dynamic due to the intrinsic complexity and chaotic behaviour of the atmospheric processes governing the weather at the regional scale. Measurements with high temporal resolution in a dense network of meteorological stations are needed to represent this variability. This is, however, not possible in most parts of the world. Consequently, data scarcity (either in time, space or both) can heavily influence model predictions.

For these reasons, it is hypothesized that satellite products such as day and night land surface temperature (LST) from MODIS can be used as a proxy for the spatio-temporal distribution of maximum and minimum air temperature. This, in turn, can be used to estimate the potential evapotranspiration (PET), for instance using the Hargreaves & Samani (1985) method. This procedure to estimate reference PET is advantageous compared to other methods (e.g. Pennman–Monteith) because it requires minimum climatological data.

The Hargreaves and Samani method estimates potential evapotranspiration E for short canopy reference as a

function of air temperature and extraterrestrial radiation:

$$E = \kappa \frac{R_a}{\lambda}(T_a + \beta)\sqrt{T_x - T_n} \tag{3}$$

where T_a, T_x and T_n denotes the average, minimum, and maximum air temperatures respectively and $\lambda = 2.45$ MJ kg^{-1} is the latent heat of vaporization of water. The ratio R_a/λ converts radiation units into equivalent water evaporation in mm d^{-1}. R_a (MJ m^{-2} d^{-1}) denotes the extraterrestrial radiation, which is estimated simply as a function of the day of the year and the latitude of the point of interest (Allen *et al.* 1998). $\kappa = 2.3 \times 10^{-3}$ is a calibration constant that approximately compensates for the differences in advection or in vapour transfer effect (Hargreaves & Samani 1985). $\beta = 17.8$ is also an empirical constant found by calibration.

Day and night MODIS LST of the pixel located closest to the meteorological station were correlated with observations of maximum and minimum air temperatures at 2 m height, respectively, for the period January–August 2001. It should be noted that this is the only period for which both kinds of observations were available. The coefficient of determination for both relationships was significant ($r^2 \sim 0.77$, p-value 0.05) as can be seen in Figures 3(b) and (c). Subsequently, the daily average temperature was estimated as the mean of both daily extremes. Proxy average T_a^{M}, minimum T_n^{M} and maximum T_x^{M} air temperatures can be estimated at any location using these relationships.

A gap-filling algorithm based on a nearest-neighbour estimator proposed by Bárdossy *et al.* (2005) was employed in the case of missing values in the time series. If MODIS LST were missing for a whole day due to cloud cover, then the long-term daily mean estimated with the observed temperatures of the meteorological station at Indore was used instead.

PET estimated with the meteorological data at Indore $E^{\mathrm{S}}(t)$ was correlated with the PET estimated with the MODIS proxy temperatures $E^{\mathrm{M}}(t)$. These variables were significantly correlated ($r^2 \sim 0.84$, p-value 0.05) as can also be seen in Figure 3(a). This result supported the hypothesis that PET based on MODIS proxy data can be used as an estimator for the reference PET based on meteorological data.

Two procedures were used in this study to estimate the spatio-temporal distribution of the PET (E) over the Mod basin due to the constraints imposed by the data availability ('Data availability' section).

1. The indirect method was used for the period in which MODIS observations were not available (i.e. 1992–2001):

$$E_i(t) = f_i(m)p(m)E^{\mathrm{S}}(t) \tag{4}$$

2. The direct method was used for the period in which MODIS observations were available (i.e. 2002–2008):

$$E_i(t) = \beta_1 + \beta_2 E(T_a^{\mathrm{M}}, T_n^{\mathrm{M}}, T_x^{\mathrm{M}})_i \tag{5}$$

The notation i represents a location index of a grid cell and t is Julian day. The index $m = 1, \ldots, 12$ represents month

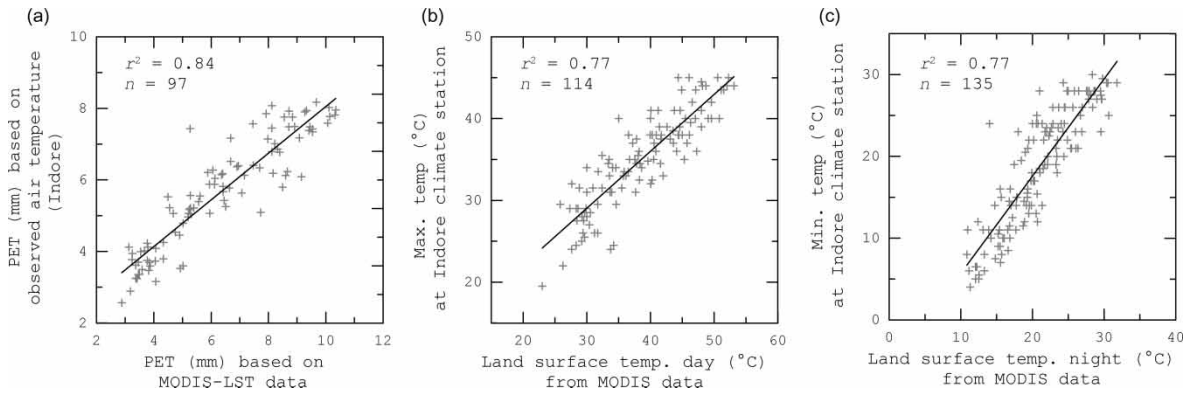

Figure 3 | (a) Relationship of the PET estimated with air temperature data and the PET obtained with daily and night land surface temperature (LST) from MODIS. PET was estimated using the Hargreaves & Samani (1985) method in both cases. (b) and (c) Relationships between maximum and minimum air temperatures at 2 m height and day and night LST, respectively. All observations correspond to the Indore metereological station for the period January–August 20018.

and β_1 and β_2 are correction factors found by regression analysis (Figure 3).

In the indirect method, the daily spatial variability of PET was reconstructed by merging a normalized long-term monthly spatial variability of PET derived from MODIS $f_i(m)$ (Equation (5)) with the temporal variability of PET estimated with the observations $E^S(t)$ (Equation (3)). $f_i(m)$ was estimated as

$$f_i(m) = \frac{\bar{E}_i^M(m)}{max\ \bar{E}^M(m)}, \quad m = 1, \ldots, 12 \tag{6}$$

where $\bar{E}_i^M(m)$ is the long-term mean PET in a given cell i at month m based on MODIS data (Equation (5)). $max\ \bar{E}^M(m)$ denotes the maximum PET over the field in a given month m. The fraction $f_i(m)$ is place-specific because PET is related to the net solar radiation which, in turn, depends on the terrain's elevation, slope and aspect (among other factors).

These intrinsic relationships were well captured by the LST from MODIS as shown in Figure 4. The temporal invariance of $f_i(m)$ at a given location i and month m over the years can be inferred from the observations at Indore as shown in Figure 5. This graph also pointed out that the annual cycle of the daily pan-evaporation is mainly the result of two recursive macroclimatic phenomena:

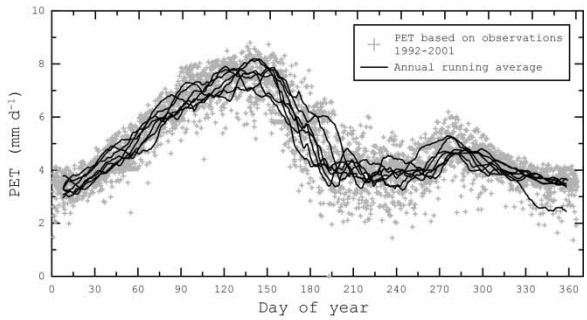

Figure 5 | Annual cycle of daily pan-evaporation at the Indore metereological station for the period 1992–2001.

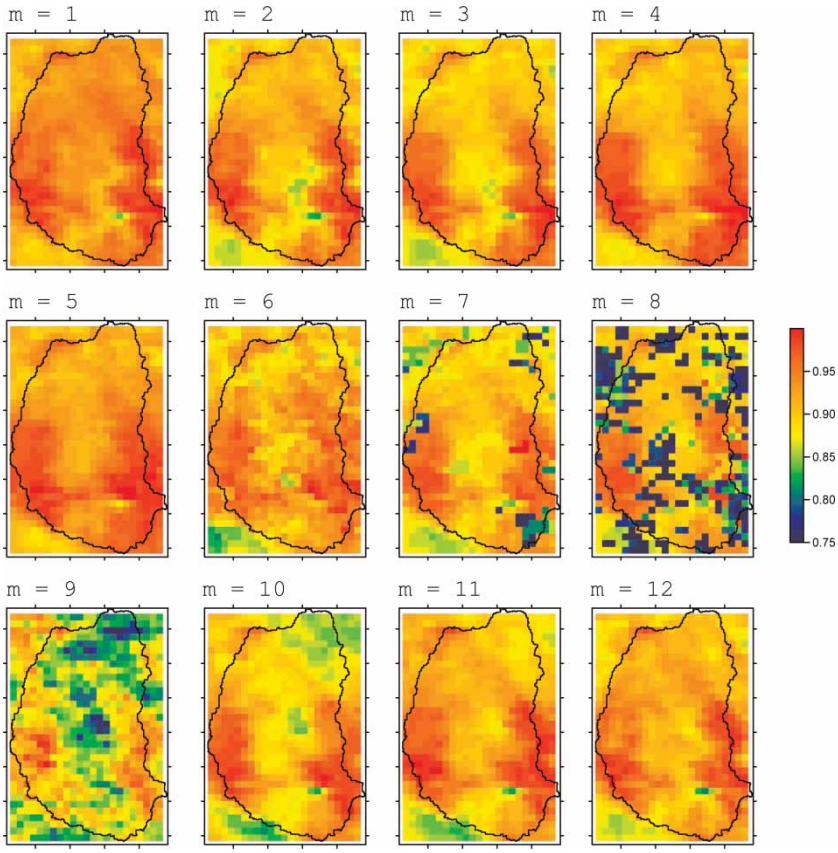

Figure 4 | Normalized spatial variability of PET (based on MODIS LST) $f_i(m)$ within the basin. Here m is an index denoting months from January to December (1–12).

(1) the southwest summer monsoon (June–September) initiated by the southeast trade winds which induces massive convective thunderstorms which bring almost 80% of the annual rainfall, and (2) the post-monsoon (October–December) governed by the influx of dry, cool and dense air masses from Central Asia.

The term $p(m)$ (Equation (4)) is a monthly varying proportionality factor that relates the long-term mean of PET obtained from MODIS with the long-term mean of PET obtained from observations. $p(m)$ was estimated as

$$p(m) = \frac{E^{\mathrm{M}}(m)}{E^{\mathrm{S}}(m)}, \quad m = 1, \ldots, 12. \tag{7}$$

Mesoscale hydrologic model

A grid-based conceptual mesoscale hydrologic model (mHM) tested in more than 30 basins in Germany (Samaniego *et al.* 2010a) was used in this study. mHM is a spatially explicit mesoscale model driven by hourly or daily forcings such as precipitation, temperature and potential evapotranspiration. It is based on numerical approximations of dominant hydrological processes that have been tested in various models: Hydrologiska Byråns Vattenbalansavdelning (HBV) (Bergström 1995) and Variable Infiltration Capacity (VIC) (Liang *et al.* 1994). This model simulates the following processes: canopy interception, snow accumulation and melting, soil moisture dynamics, infiltration and surface runoff, evapotranspiration, subsurface storage and discharge generation, deep percolation and baseflow and discharge attenuation and flood routing. A schematic representation of mHM is depicted in Figure 6. Readers may refer to Samaniego *et al.* (2010b) for a detailed model description.

mHM was implemented as lumped and distributed versions. The lumped version does not take into account the spatial variability of meteorological forcings, parameters and state variables shown in Figure 6; the distributed version does. The lumped model can therefore be considered as the limit of the distributed model in which the cell size is chosen in order to cover the whole basin with a single grid cell.

A distributed model requires fields of effective parameters which have to be estimated through calibration. The lack of sufficient data in poorly gauged basins may hinder this inference process, however. A disadvantage of these types of models is that they quickly tend to become over-parameterized due to the large number of free parameters (Kirchner 2006). Regionalization techniques have been pursued in hydrological modelling to overcome this problem.

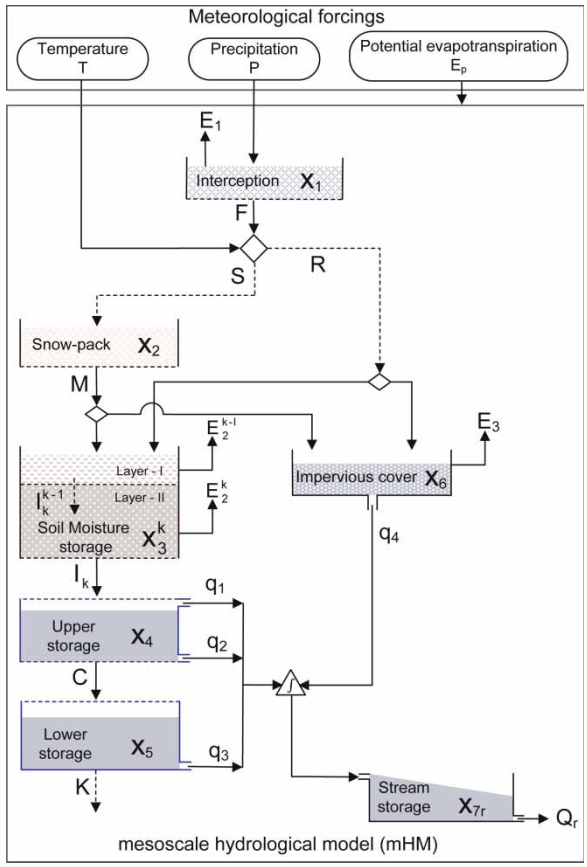

Figure 6 | Schematic representation of different components accounted in the distributed mHM version where X is state variable, E is actual evapotranspiration, q is component of runoff, S is snow precipitation depth, R is rain precipitation depth, F is throughfall, I is infiltration capacity, C is percolation, K is gain/loss flux in a leaking cell and Q_r is net runoff produced at the outlet of a grid cell.

Multiscale parameter regionalization

There are many regionalization techniques reported in literature (Abdulla & Lettenmaier 1997; Hundecha & Bárdossy 2004; Pokhrel *et al.* 2008; Samaniego *et al.* 2010b). A review of the advantages and disadvantages of these techniques is outwith the scope of this study. Interested readers may refer to Samaniego *et al.* (2010b) for a comparative analysis of existing regionalization techniques. Their main shortcoming,

however, is the lack of sub-grid variability of basin descriptors and parameters. The sub-grid parameter variability in regionalization techniques is fundamental to ensure the closure of water mass balance at any control volume as well as to facilitate the transferability of parameters from a gauged to an ungauged basin (Entekhabi & Eagleson 1989; Ghan *et al.* 1997; Arora *et al.* 2001; Samaniego *et al.* 2010a, b). Multi-scale parameter regionalization (MPR) proposed by Samaniego *et al.* (2010b) was applied in this study to explicitly address these problems.

Based on MPR, model parameters at a coarser scale (level 1, say 1 km), in which dominant hydrological processes are represented, are linked with their corresponding parameters at a finer resolution (level 0, say 100 m), in which the morphologic and land cover datasets (e.g. Digital Elevation Model or DEM from Landsat images) are available. The linkage is made by upscaling operators such as the harmonic mean and the geometric mean, among others. The general form of an upscaling operator is:

$$\beta_{ki}(t) = O_k\langle\beta_{kj}(t) \quad \forall j \in i_i\rangle_i \tag{8}$$

where

$$\beta_{kj}(t) = f_k(u_j(t), \gamma). \tag{9}$$

Here $O_k\langle\bullet\rangle_i$ denotes the type of operator applied for the regionalization of the parameter k. β_{kj} denote model parameters at the finer scale which are, in turn, regionalized with catchment descriptors through non-linear transfer functions f_k ($k = 1, \ldots, K$ where K is the number of distributed model parameters). γ is an n-dimensional vector of spatially invariant global parameters. u_j denotes a γ-dimensional predictor vector for cells j at level 0 which are contained by cell i at level 1.

This technique has been tested and cross-validated in several river basins located in Germany (Samaniego *et al.* 2010a). Results of this study indicate that MPR is an effective way to reduce over-parameterization and hence predictive uncertainty of model outputs. Cross-validation tests also indicated that the transferability of the global parameters obtained with this technique to other basins is possible (Samaniego *et al.* 2010b).

In particular, mHM requires $K = 28$ parameters per cell to account for the spatial variability of the dominant hydrological processes. Calibrating this model for every grid cell with a significant number of free parameters would lead to over-parameterization (i.e. $K\times$ number of modelling cells). This in turn would tend to increase the predictive uncertainty of model outputs (Schulz *et al.* 2001). Applying the MPR technique as indicated in Table 1, on the contrary, would require only $n = 61$ global parameters γ inferred through calibration.

Process understanding and empirical evidence are used to define the *a priori* relationships represented in Equation (9). *A priori* ranges for global parameters were found through literature survey (e.g. typical pedo-transfer functions coefficients). If these ranges were not known in advance, then large variability ranges were set up for the model calibration. Additionally, global parameters found in gauged basins were taken as *a priori* estimates (Samaniego *et al.* 2010a).

Effects of the sub-grid variability

A numerical experiment was carried out to visualize the effect of the sub-grid variability on effective model parameters and state variables. The simplest way to show the effects of upscaling parameters or predictors is by reversing the regionalization procedure given by Equations (8) and (9). In other words, first estimate effective predictors at level 1 (e.g. soils texture characteristics) and then apply regionalization function Equation (9). Note that the effective predictors are generally estimated within GIS systems and often with inappropriate algorithms (e.g. arithmetic mean). Since this method is quite common in hydrological studies, it is referred to as the 'standard regionalization procedure' (SR) (Hundecha & Bárdossy 2004; Pokhrel *et al.* 2008).

Upscaling regionalized parameters from the sub-grid scale to the modelling scale instead of regionalizing parameters at the modelling scale with upscaled predictors leads to different results (as shown in Figure 7) due to non-linearities implicit in the hydrologic model and regionalization functions. In this example, the spatial distribution of the effective soil porosity and soil water content obtained with the standard regionalization approach at (2×2) km (level 1) clearly underestimates soil porosity within the

Table 1 | List of mHM model parameters

Param.	Description	Pred. Var.	U. Oper.
β_1	Thickness of waterfilm on the canopy surface (–)	Land cover	*A*
β_2	Threshold temperature for phase transition snow and rain (°C)	–	–
β_3	Degree-day factor during rainless days (mm d^{-1} °C)	Land cover	*A*
β_4	Rate of increase of the degree-day factor per unit of precipitation (mm d^{-1} °C)	–	–
β_5	Max. degree-day factor reached during rainy days (mm d^{-1} °C)	Land cover	*A*
β_6^k	Max. soil moisture content of *k*th root zone layer (mm)	Soil texture, land cover	*H*
β_7	Parameter that determines the relative contribution of rain or snowmelt to runoff (–)	Soil texture, land cover	*H*
β_8	Critical value of soil ice content in first root zone layer above which the soil is practically impermeable (mm)	Soil texture, land cover	*H*
β_9	Shape factor of the gamma distribution that statistically estimates the virtual impermeable area due to frozen soil (–)	–	–
β_{10}	Antecedent Temperature Index (ATI, proxy for soil temperature) threshold below which unfrozen water content reaches its minimum value (K)	Soil texture	*H*
β_{11}	ATI threshold above which no frozen water exists (K)	Soil texture	*H*
β_{12}	Min. value of unfrozen water content estimated as the fraction of total water content of first root zone layer (–)	Soil texture	*H*
β_{13}	Weighting multiplier to estimate ATI from air temp (–)	–	–
β_{14}	Max. ponding retention in impervious areas (mm)	Land cover	*A*
β_{15}	Permanent wilting point, estimated as the fraction of maximum soil moisture content (–)	Soil texture, land cover	*H*
β_{16}	Soil moist. limit above which the actual evapotrans. is equated with the potential evapotransp., estimated as the fraction of maximum soil moisture content (–)	Soil texture, land cover	*H*
β_{17}	Fraction of roots in the first root zone layer (–)	Land cover	*A*
β_{18}	Max. water holding capacity of the unsat. zone (mm)	Soil texture, land cover	*H*
β_{19}	Fast recession constant (d)	Slope	*A*
β_{20}	Slow recession constant (d)	Soil texture	*A*
β_{21}	Exponent that quantifies the degree of non-linearity of the cell response (–)	Soil texture	*A*
β_{22}	Effective percolation rate (d)	Soil texture	*A*
β_{23}	Baseflow recession rate (d)	Geology	*M*
β_{24}	Fraction of the groundwater recharge that might be gained or lost either as deep percolation or as intercatchment groundwater flow in non-conservative catchments (–)	Geology	*M*
β_{25}	Duration of triangular unit hydrograph (h)	Length, slope and land cover along drainage path within cell	*G*
β_{26}	Muskingum travel time parameter (h)	Length, slope and land cover of river reach	–
β_{27}	Muskingum attenuation parameter (–)	Slope of river reach	–
β_{28}	Aspect correction factor of the PET (–)	Aspect	*A*

The predictor variables and the corresponding upscaling operator (arithmetic mean *A*, harmonic mean *H*, geometric mean *G* and majority statistic *M*) for the MPR method are shown. Soil textural data includes the percentage of sand and clay content and rootzone depth, whereas land cover is grouped in three classes: forest, impermeable and permeable cover. For more details refer to Samaniego *et al*. (2010b).

Mod basin, taking the soil porosity estimated at level 0 (100×100) m as a reference. As a result, state variables simulated by the mHM such as soil moisture (x_3 in Figure 6) were clearly underestimated during dry and wet periods.

DESCRIPTION OF NUMERICAL EXPERIMENTS

Three numerical experiments were carried out to address the research questions proposed in the Introduction.

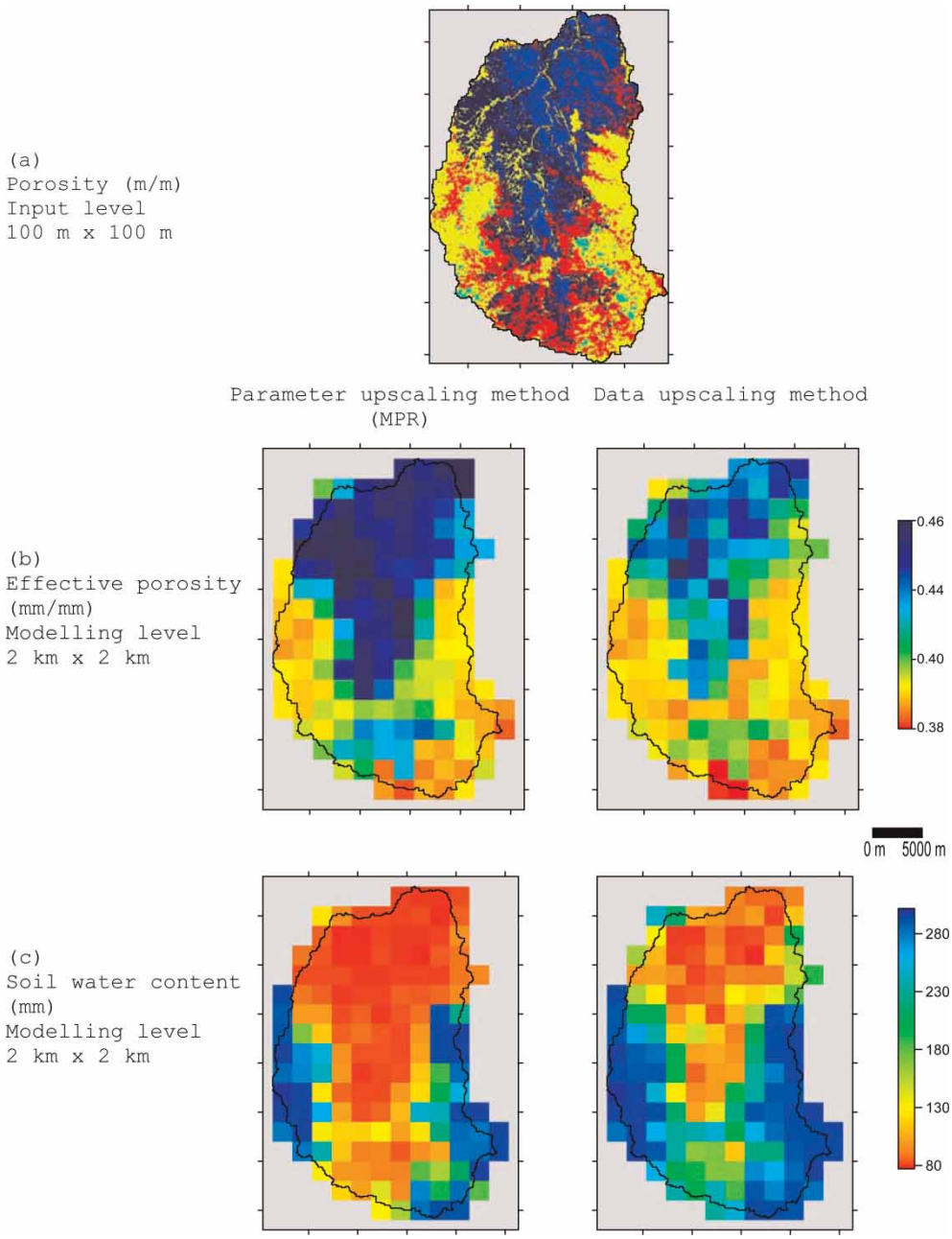

Figure 7 | Variability of an effective model parameter (soil porosity) and a state variable (soil water content) when the subgrid variability of the predictors is either MPR or SR. (a) Soil porosity at input data level (100 m × 100 m) estimated with a pedotransfer function used as reference. (b) Effective soil porosity at modelling scale (2 km × 2 km) obtained by MPR (left) and SR methods (right). (c) Soil water content obtained with MPR and SR methods, respectively.

Experiment 1: The purpose of this experiment was to assess the efficiency of the distributed version of mHM compared to its lumped version. The selected calibration period was 1992–1996, in which streamflow data were available. Precipitation and PET were estimated based on observations at meteorological stations using procedures described in the 'Blending remote sensing data' section. The spin-up period was from January to March 1992. The initial soil moisture conditions were unknown but it can be assumed that they were quite dry before the monsoon. One hundred realizations of model runs were carried out to investigate the model sensitivity to the initial soil moisture conditions.

Experiment 2: The purpose of this experiment was to investigate the feasibility of using TRMM data as a proxy of interpolated precipitation data for streamflow predictions. Two variants of the forcings were employed. The first uses precipitation interpolated with EDK from 1992 to 2000. This run was used as a reference because no discharge observations are available after 1997. The second variant differs from the former in the precipitation forcings after 1997. In this case only TRMM fields were used. PET was derived with the indirect method described in the 'Blending remote sensing data' section and was kept similar in both variants.

Experiment 3: The purpose of this experiment was to evaluate the plausibility of driving mHM with only satellite-based products. Two issues were investigated in this context: (1) the effect of spin-up mHM with meteorological information before the satellite data is used, and (2) the effect of initial soil moisture conditions when only remotely sensed products are used. Two simulation settings were conducted to attain these goals. In the first, mHM was initialized with random initial soil moisture conditions and then driven by the interpolated station data for the period from 1992 to 1997. Afterwards, mHM was forced until 2008 with only satellite data, i.e., TRMM precipitation and PET based on the MODIS LST ('Blending remote sensing data' section). These simulations were used as a control run. In the second simulation setting, mHM was started with random soil moisture conditions in 1998 and then forced with satellite data until the end of 2008. Global model parameters were kept identical in all simulations.

RESULTS AND DISCUSSION

Experiment 1

The following procedure was implemented to test the null hypothesis that a lumped model is adequate to simulate river discharge in a data-sparse semi-arid basin. The alternative hypothesis was that a regionalized distributed hydrologic model would be more efficient than the lumped model version given the same data conditions.

All parameters for the lumped version of mHM were found through automatic optimization since no *a priori* parameter estimates were available. Simulated annealing (Aarts & Korst 1990) was used as an optimization algorithm to maximize the Nash–Sutcliffe efficiency (NSE) estimated with simulated and observed daily values during the period 1992–1996. The best fit obtained for the lumped model version had a NSE $= -0.20$, i.e., a very poor performance. A negative NSE value clearly indicated that a lumped model version was not able to simulate daily streamflow in this semi-arid basin. Furthermore, this result also highlighted that additional model complexity would be required to better account for the observed streamflow dynamics.

Subsequently, *a priori* estimates of global parameters obtained in gauged basins (Samaniego *et al.* 2010a) were used to set up the distributed version of mHM. The Nash–Sutcliffe efficiency between daily simulated and observed discharges in the same period of time was 0.20. This was a satisfactory result considering that the distributed model version was not automatically calibrated as in the case of the lumped model. NSE was further increased to 0.25 by manually fine-tuning two global parameters that are related to slow interflow and baseflow model parameters (β_{20} and β_{23}).

The low NSE obtained with the distributed model version might be an indication of data quality issues. For instance, it was noticed that the daily discharge hydrograph during the high-flow period (i.e. the monsoon) exhibited large fluctuations that could not always be explained with the observed precipitation patterns: i.e., exceptional large discharge values observed when little precipitation was recorded in the days before such event. There are many possible reasons for this mismatch. The most likely are estimation errors and malfunctioning of either the streamflow or the

rainfall gauges. It is not possible, however, to conclude which source of error is the most likely at this stage. Monthly discharge was therefore preferred to analyze model performance since it minimized the influence of outliers.

The coefficient of determination between simulated and observed monthly discharge obtained with the distributed version of mHM ($r^2 \sim 0.55$) was 22% greater than that obtained with the lumped version ($r^2 \sim 0.45$). The best fit between the observed and the simulated streamflow was obtained with the distributed version as can be seen in Figures 8(a) and (b). The root mean squared errors obtained for both models were 67 and 84 $m^3 s^{-1}$, respectively. Thus, the distributed model version was better suited to describe the streamflow dynamics of the Mod basin, which is mainly driven by annual monsoon events. The lumped model version, on the contrary, was unable to reproduce the low-flow conditions observed in this basin after the monsoon. These results highlighted a significant advantage of the distributed model version over the lumped version. These results corroborated similar findings reported by Michaud & Sorooshian (1994) in other semi-arid basins.

Additionally, the sensitivity of the simulated discharge with respect to the initial state of the soil water content was also investigated in this experiment. Each model version was initialized in January 1991 with plausible random values of soil moisture for the dry season to achieve this goal. The variability of the simulated monthly streamflow is also depicted in Figures 8(a) and (b). These results indicated that both model versions were extremely sensitive to the initial soil water content, but the variability decreased over time. At least 3 years of spin-up time was required by the distributed model version to catch up with the natural long-term discharge dynamics of the Mod basin. These results also indicated that the lumped model version exhibited a higher sensitivity to the initialization conditions than the distributed version.

Experiment 2

The reliability of the TRMM data to make hydrological predictions in the Mod basin could only be made during the period from 1998 to 2000 when both precipitation observations and TRMM were available. Unfortunately, there were no discharge observations during this period. Because of this, a monthly discharge simulation obtained with the distributed model version with the best NSE was used as a reference run for the period from 1998 to 2001.

The following procedure was implemented to test the null hypothesis that TRMM is not a reliable input driver for mHM. Two runs were set up, differing from each other only in the forcings used from 1998 to 2000 namely: the control run (i.e. EDK-best) used interpolated data whereas the test run (i.e. EDK + TRMM) used TRMM data. Both runs used the same parameterization (the best found), input data and initial conditions. The spin-up period was set up from 01/03/1992 until 31/12/1997. PET was obtained based on station information and MODIS data as described in the 'Blending remote sensing data' section.

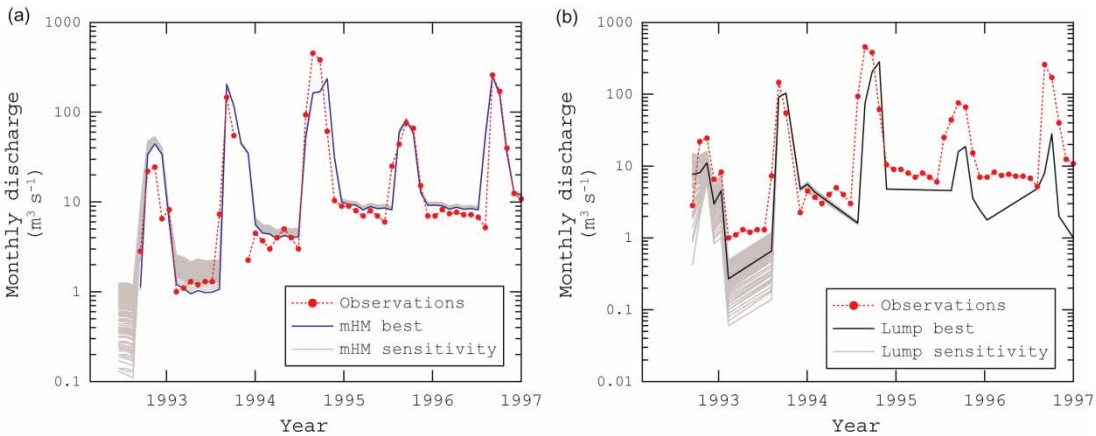

Figure 8 | Comparison of model performance using the (a) distributed and (b) lumped versions of mHM. Both model versions were forced with the same interpolated precipitation data (EDK) during the calibration period (1992–1997). Model sensitivity to the initial soil moisture conditions is also depicted.

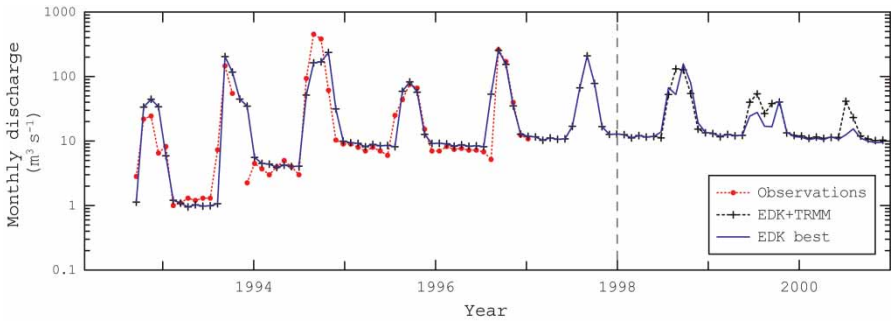

Figure 9 | Comparison of model simulations using two precipitation products (EDK and TRMM). The control run (EDK best) employed interpolated data from 1992 to 2000. The evaluation run (EDK + TRMM) was first initialized with interpolated data (EDK) from 1992 to 1997 and then forced with TRMM data from 1998 to 2000.

Results of this experiment are shown in Figure 9. The coefficient of determination obtained between the control and test simulations was $r^2 \sim 0.58$ for the period 1998–2000. The simulations were almost similar for the low-flow regime of the Mod basin. Monthly high-flow discharges obtained with both simulations were quite similar for the monsoon of 1998. From 1999 onwards, however, high flows estimated with interpolated rainfall data became significantly smaller than those obtained with TRMM. This divergence may have originated from a malfunction of the raingauges, a lack of spatial coverage and/or a lack of maintenance.

The overestimation of TRMM over interpolated precipitation is likely because available rainfall gauges did not measure rainfall values less than 1 mm, whereas satellite data indicated that small amounts of rainfall did occur. These discrepancies induced a significant difference in the lower tail of the distribution functions of TRMM and EDK interpolated precipitation as shown in Figure 10. During the period from 1998 to 2000, the annual precipitation estimated by TRMM was on average 9% greater than that estimated with the raingauges.

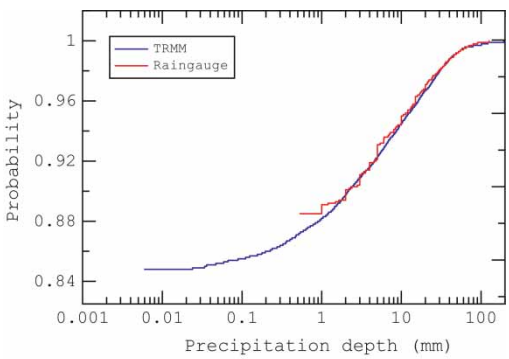

Figure 10 | Empirical probability density functions of observed precipitation at the Indore meteorological station and the corresponding TRMM for the period from 1998 to 2000.

The flow duration curve (Figure 11(a)) obtained with the distributed version exhibited a relatively good agreement with that obtained with the observations during the period 1992–1997. The model systematically underestimated the observed high-flow values. As expected, the flow duration curves obtained with control and test simulations for the period 1998 to 2000 showed that the streamflow simulated with TRMM data tended to be greater than that estimated with the interpolated data (EDK), especially for events which were on average equalled or exceeded 30% of the time.

Given the large uncertainty of the discharge and meteorological data in this basin, it could not be concluded whether these errors were the result of either deficiencies in the model structure and its parameterization or measurement errors, or both. It is conceivable, nevertheless, to state that a large part of this bias might originate due to discharge measurement errors considering the harsh conditions of this rural area, the intermittency of the existing time series and the relatively good agreement between simulated discharge obtained from 1998 to 2000 with TRMM and EDK interpolations (Figure 9).

Consequently, it is possible to conclude that TRMM precipitation can be used as a driver of mHM (i.e. the null hypothesis can be rejected) provided that the model was previously warmed-up with at least 3 years of observed precipitation. The consequence of not fulfilling this initialization condition is detailed below.

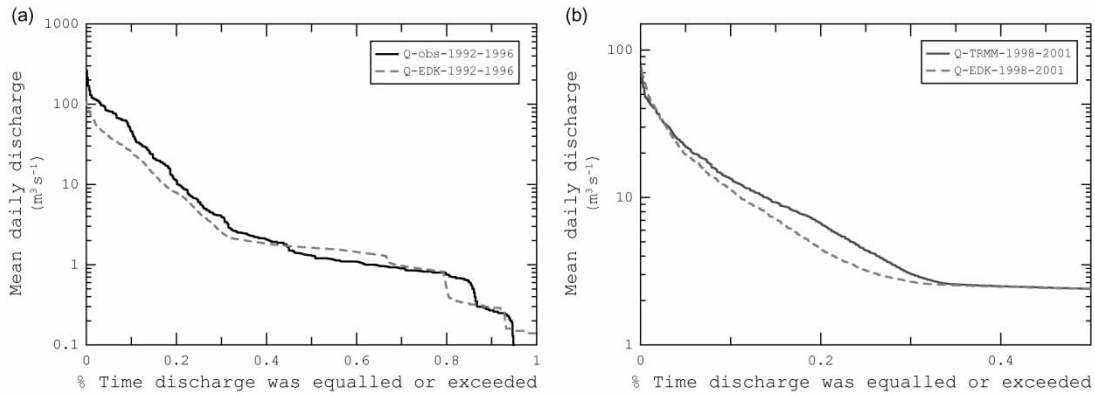

Figure 11 | (a) Observed and simulated (mHM) flood duration curves for the period from 1992 to 1997. (b) Flood duration curves obtained using TRMM precipitation fields and that obtained by interpolating raingauge data for the period 1998 to 2000.

Experiment 3

The main goal of this experiment was to investigate under which conditions remotely sensed data can be used for streamflow predictions in ungauged or in poorly gauged basins. The null hypothesis in this case was that the model initialization conditions and *in situ* data did not contribute significantly to improve model predictions. Two simulations were carried out to test this hypothesis. The first was denoted as the control run. This run was forced with interpolated data from 1992 to 1997 and then with TRMM precipitation and MODIS-based PET until 2008. The best possible parameterization and initial soil moisture conditions corresponding to the best NSE value for the period

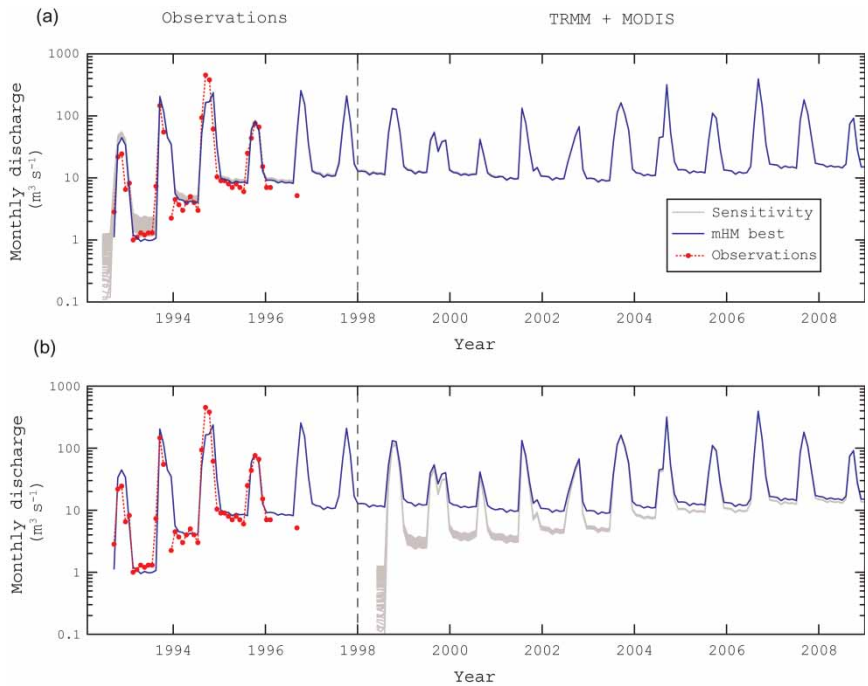

Figure 12 | Effects of the spin-up period with *in situ* observations and the initial soil moisture conditions on model output. In both panels the control run (blue) was initialized with interpolated data from 1992 to 1997 and trained to reproduce available discharge observations. Afterwards, the model was forced with TRMM data until the end of 2008. (a) Spin-up period from 1992 to 1997 using interpolated data. From 1998 to 2008 the model was forced with satellite data. (b) No spin-up period used; the model was driven only with satellite products.

1992–1996 were used for this run (denoted 'mHM best' in Figure 12(a)). The second simulation was denoted as the test run. This was started in 01/03/1998 and then forced until the end of 2008 with the TRMM precipitation and the MODIS-based PET only.

One hundred different replicates of both simulations using randomly selected initial soil water content conditions and slightly different parameterizations were carried out to emphasize possible differences from the control run simulation.

Results of the control run (Figure 12(a)) indicated that the simulated discharge is quite sensitive to initial soil moisture during the starting phase of the simulation (i.e. the first 3 years). Afterwards, simulated streamflow became insensitive to this factor. The control run simulation after 1998 (purely satellite-based forcings) exhibited a cyclic behaviour whose amplitude, on average, was similar to that obtained with interpolated rainfall from 1994 to 1998.

The low-flow discharge regime obtained with the test run, on the contrary, exhibited a significant sensitivity to initial conditions (Figure 12(b)). This effect, however, tended to become insignificant (i.e. convergence reached) only after 10 years from the starting point. These results demonstrated the importance of initializing the model with measured data for at least a couple of years before the model is forced with satellite-based data. High-flow estimates, on the contrary, did not exhibit much sensitivity to the initial soil water content.

CONCLUSIONS

In this study two remotely sensed products (TRMM precipitation and MODIS-LST) were used to drive lumped and distributed versions of the hydrologic model mHM in a poorly gauged basin in northwest India.

The application of a distributed model in a data-sparse region was possible because model parameters of mHM were regionalized, which allowed us to use *a priori* estimates of global parameters obtained in other gauged basins. Additionally, the importance of accounting for the sub-grid parameter variability to estimate effective parameters and its effect on simulated soil moisture was also shown.

Simulation results showed that a distributed hydrologic model with regionalized parameters would help to reduce the model bias by at least 20% with respect to the spatially lumped version in this semi-arid region. This reduction in bias, in turn, contributed to significantly increased model efficiency.

Blending satellite information with observed meteorological data enabled us to apply the distributed model in the Mod basin. It was also shown that TRMM precipitation can be used in hydrological studies when no meteorological data is available, provided that the model spin-up time is at least 10 years. The results also indicated that MODIS LST can be used as a proxy to derive PET as long as regionalization functions to estimate maximum and minimum air temperature are available. Additional research is still required to estimate the uncertainty of discharge statistics required for planning purposes.

The role of the initial conditions and the spin-up period must be carefully taken into account, especially if the model is only driven with satellite-based data. In this case, the model would take at least twice as long to converge to the state reached by a model forced with measured data. Consequently, short spin-up periods would lead to biased simulations.

REFERENCES

Aarts, E. & Korst, J. 1990 *Simulated Annealing and Boltzmann Machines: A Stochastic Approach To Combinatorial Optimization And Neural Computing*. Wiley, Chichester.

Abdulla, F. & Lettenmaier, D. 1997 Development of regional parameter estimation equations for a macroscale hydrologic model. *J. Hydrol.* **197**, 230–257.

Allen, R., Pereira, L., Raes, D. & Smith, M. 1998 Crop evapotranspiration: guidelines for computing crop water requirements. FAO Irrigation and Drainage Paper 56. FAO (Food and Agriculture Organization of the United Nations), Rome.

Arora, V. K., Chiew, F. H. S. & Grayson, R. B. 2001 Effect of sub-grid-scale variability of soil moisture and precipitation intensity on surface runoff and streamflow. *J. Geophys. Res.* **106** (D15), 17073–17091.

Bárdossy, A. 2007 Calibration of hydrological model parameters for ungauged catchments. *Hydrol. Earth Syst. Sc.* **11** (2), 703–710.

Bárdossy, A., Pegram, G. S. & Samaniego, L. 2005 Modeling data relationships with a local variance reducing technique: Applications in hydrology. *Water Resour. Res.* **41**, W08404.

Bergström, S. 1995 The HBV model. In: *Computer Models of Watershed Hydrology* (V. Singh, ed.). Water Resources Publications, Colorado, USA, pp. 443–476.

Deutsch, C. & Journel, A. 1998 *GSLIB: Geo Statistical Software Library and User's Guide*. 2nd edition, Oxford University Press, New York.

Entekhabi, D. & Eagleson, P. S. 1989 Land surface hydrology parameterization for atmospheric general circulation models including subgrid scale spatial variability. *J. Climate* **2**, 816–831.

Gebremichael, M., Krajewski, W. F., Morrissey, M., Langerud, D., Huffman, G. J. & Adler, R. 2003 Error uncertainty analysis of GPCP monthly rainfall products: a databased simulation study. *J. Appl. Meteorol.* **42** (12), 1837–1848.

Geological Survey of India (GSI) 1978 Calcutta National Bureau of Soil Survey and Land Use Planning. Available from: http://www.gsi.gov.in (accessed 11 December 2009).

Ghan, S. J., Liljegren, J. C., Shaw, W. J., Hubbe, J. H. & Doran, J. C. 1997 Influence of subgrid variability on surface hydrology. *J. Climate* **10** (12), 3157–3166.

Hargreaves, G. H. & Samani, Z. A. 1985 Reference crop evapotranspiration from temperature. *Appl. Eng. Agric.* **1**, 96–99.

Hilker, T., Wulder, M. A., Coops, N. C., Seitz, N., White, J. C., Gao, F., Masek, J. G. & Stenhouse, G. 2009 Generation of dense time series synthetic Landsat data through data blending with MODIS using a spatial and temporal adaptive reflectance fusion model. *Remote Sens. Environ.* **113** (9), 1988–1999.

Hossain, F. & Huffman, G. J. 2008 Investigating error metrics for satellite rainfall data at hydrologically relevant scales. *J. Hydrometeorol.* **9** (3), 563–575.

Hundecha, Y. & Bárdossy, A. 2004 Modeling effect of land use changes on runoff generation of a river basin through parameter regionalization of a watershed model. *J. Hydrol.* **292**, 281–295.

Jackisch, C. 2007 Towards Applied Modeling of the Human-Eco-System: an approach of hydrology based integrated modeling of a semi-arid sub-catchment in rural north-west India. Masters thesis, University of Potsdam, Germany.

Joyce, R. J., Janowiak, J. E., Arkin, P. A. & Xie, P. 2004 CMORPH: a method that produces global precipitation estimates from passive microwave and infrared data at high spatial and temporal resolution. *J. Hydrometeorol.* **5**, 487–503.

Kirchner, J. W. 2006 Getting the right answers for the right reasons: Linking measurements, analyses, and models to advance the science of hydrology. *Water Resour. Res.* **42** (3), W03S04.

Liang, X., Lettenmaier, D. P., Wood, E. F. & Burges, S. J. 1994 A simple hydrologically based model of land-surface water and energy fluxes for general-circulation models. *J. Geophys. Res.-Atmos.* **99** (D7), 14415–14428.

McIntyre, N., Lee, H., Wheater, H., Young, A. & Wagener, T. 2005 Ensemble predictions of runoff in ungauged catchments. *Water Resour. Res.* **41**, W12434.

Michaud, J. & Sorooshian, S. 1994 Comparison of simple versus complex distributed runoff models on a mid-sized semiarid watershed. *Water Resour. Res.* **30** (3), 593–605.

Oudin, L., Andreassian, V., Perrin, C., Michel, C. & LeMoine, N. 2008 Spatial proximity, physical similarity, regression and ungaged catchments: a comparison of regionalization approaches based on 913 French catchments. *Water Resour. Res.* **44**, W03413.

Pan, M., Li, H. & Wood, E. 2010 Assessing the skill of satellite-based precipitation estimates in hydrologic applications. *Water Resour. Res.* **46**, W09535.

Pokhrel, P., Gupta, H. V. & Wagener, T. 2008 A spatial regularization approach to parameter estimation for a distributed watershed model. *Water Resour. Res.* **44**, W12419.

Reed, S., Koren, V., Smith, M., Zhang, Z., Moreda, F., Seo, D.-J. & Participants, D. 2004 Overall distributed model intercomparison project results. *J. Hydrol.* **298** (1–4), 27–60.

Samaniego, L., Bárdossy, A. & Kumar, R. 2010a Streamflow prediction in ungauged catchments using copula-based dissimilarity measures. *Water Resour. Res.* **46**, W02506.

Samaniego, L., Kumar, R. & Attinger, S. 2010b Multiscale parameter regionalization of a grid-based hydrologic model at the mesoscale. *Water Resour. Res.* **46**, W05523.

Schulz, K., Jarvis, A., Beven, K. & Soegaard, H. 2001 The predictive uncertainty of land surface fluxes in response to increasing ambient carbon dioxide. *J. Climate* **14** (12), 2551–2562.

Sivapalan, M., Takeuchi, K., Franks, S., Gupta, V., McDonnell, J., Mendiondo, E., O'Connell, P., Oki, T., Pomeroy, J. W., Schertzer, D., Uhlenbrook, S. & Zehe, E. 2003 IAHS decade on predictions in ungauged basins (PUB), 2003–2012: Shaping an exciting future for the hydrological sciences. *Hydrolog. Sci. J.* **48** (6), 867–880.

Solomon, S., Qin, D., Manning, M., Chen, Z., Marquis, M., Averyt, K., Tignor, M. & Miller, H. (eds.) 2007 *Climate change 2007: The Physical Science Basis*. Contribution of Working Group I to the Fourth Assessment Report of the Intergovernmental Panel on Climate Change, Cambridge University Press, Cambridge.

Tobin, K. J. & Bennett, M. E. 2010 Adjusting satellite precipitation data to facilitate hydrologic modeling. *J. Hydrometeorol.* **11**, 966–978.

Vorosmarty, C. 2001 Global water data: a newly endangered species. *Eos Trans. AGU* **82** (5), 54.

Wagener, T. & Wheater, H. S. 2006 Parameter estimation and regionalization for continuous rainfall-runoff models including uncertainty. *J. Hydrol.* **320** (1–2), 132–154.

Xia, Y., Pitman, A. J., Gupta, H. V., Leplastrier, M., Henderson-Sellers, A. & Bastidas, L. A. 2002 Calibrating a land surface model of varying complexity using multicriteria methods and the cabauw dataset. *J. Hydrometeorol.* **3** (2), 181–194.

First received 3 April 2011; accepted in revised form 31 August 2010. Available online June 2011